Universal defect density scaling in an oscillating dynamic phase transition

Wei-Can Yang [1], Makoto Tsubota [1,2,*] Adolfo del Campo [3,4,†] and Hua-Bi Zeng [5,6,‡]

[1]*Department of Physics, Osaka Metropolitan University, 3-3-138 Sugimoto, 558-8585 Osaka, Japan*

[2]*Nambu Yoichiro Institute of Theoretical and Experimental Physics (NITEP), Osaka Metropolitan University, 3-3-138 Sugimoto, Sumiyoshi-ku, Osaka 558-8585, Japan*

[3]*Department of Physics and Materials Science, University of Luxembourg, L-1511 Luxembourg, Luxembourg*

[4]*Donostia International Physics Center, E-20018 San Sebastián, Spain*

[5]*Center for Theoretical Physics, Hainan University, Haikou 570228, People's Republic of China*

[6]*Center for Gravitation and Cosmology, College of Physical Science and Technology, Yangzhou University, Yangzhou 225009, China*

Universal scaling laws govern the density of topological defects generated while crossing an equilibrium continuous phase transition. The Kibble-Zurek mechanism (KZM) predicts the dependence on the quench time for slow quenches. By contrast, for fast quenches, the defect density scales universally with the amplitude of the quench. We show that universal scaling laws apply to dynamic phase transitions driven by an oscillating external field. The difference in the energy response of the system to a periodic potential field leads to energy absorption, spontaneous breaking of symmetry, and its restoration. We verify the associated universal scaling laws, providing evidence that the critical behavior of nonequilibrium phase transitions can be described by time-average critical exponents combined with the KZM. Our results demonstrate that the universality of critical dynamics extends beyond equilibrium criticality, facilitating the understanding of complex nonequilibrium systems.

I. INTRODUCTION

The Kibble-Zurek Mechanism (KZM) provides a universal paradigm for the description of critical phenomena exhibited by complex systems during spontaneous symmetry breaking [1–3]. This mechanism describes the formation of long-lived topological defects when a system undergoes a continuous or quantum phase transition across a critical point at a finite rate. While in its genesis it aimed at describing structure formation in a cosmology [1], the KZM has been generalized to include condensed matter system and various other scenarios [2–10]. Its broad applicability has made it an invaluable tool for studying phase transitions and understanding the dynamics of critical phenomena in classical and quantum systems.

Consider a system with a continuous phase transition at the critical point λ_c. In terms of the control parameter λ, we define a reduced distance parameter $\epsilon = 1 - \lambda/\lambda_c$ that then governs the divergence of the equilibrium correlation length ξ and the equilibrium relaxation time τ,

$$\xi = \frac{\xi_0}{|\epsilon|^\nu}, \quad \tau = \frac{\tau_0}{|\epsilon|^{z\nu}}, \tag{1}$$

where ν and z are the correlation length and dynamic critical exponent, respectively. Both ν and z depend on the dimensionality and symmetry of the order parameter and are

universal, i.e., independent of the microscopic details of the system [11].

When the control parameter is driven in time, near the critical point λ_c, critical slowing down prevents the system from adapting to the instantaneous equilibrium configuration for $\lambda(t)$, effectively freezing the system. KZM characterizes the nonequilibrium state resulting from a linearized quench with $\lambda(t) = \lambda_c[1 - \epsilon(t)]$ and $\epsilon(t) = t/\tau_Q$. It makes use of the freeze-out time $\hat{t}$, estimated by comparing the relaxation time with the time gone by after crossing the critical point $\hat{t} = \tau(\hat{t}) = \tau_0/|\epsilon(\hat{t})|^{z\nu}$, which yields $\hat{t} \sim \tau_0(\tau_Q/\tau_0)^{z\nu/(1+z\nu)}$. KZM predicts that domains form with an average size set by the equilibrium correlation length at the freeze-out time, $\hat{\xi} = \xi[\hat{\epsilon}] = \xi_0(\tau_Q/\tau_0)^{\nu/(1+z\nu)}$. As a result, the average number of pointlike topological defects in a d-dimensional system scales as

$$n \sim \frac{1}{\hat{\xi}^d} \sim \tau_Q^{-\frac{d\nu}{1+z\nu}}. \tag{2}$$

This universal scaling law predicts the relationship between the topological defects and the quench rate in systems across vastly different scales, from cosmological scenarios to quantum phase transitions. Supporting evidence has been found in many experiments [3] using liquid crystals [4,12], superfluid helium [13–15], ultracold gases [8,16,17], and programmable quantum devices [18–22]. While many of these experiments concern pointlike defects, the KZM has also been verified in the formation of Ising domains [23].

KZM was conceived to describe the dynamics across an equilibrium phase transition, combining equilibrium scaling relations with the driving of the control parameter. However,
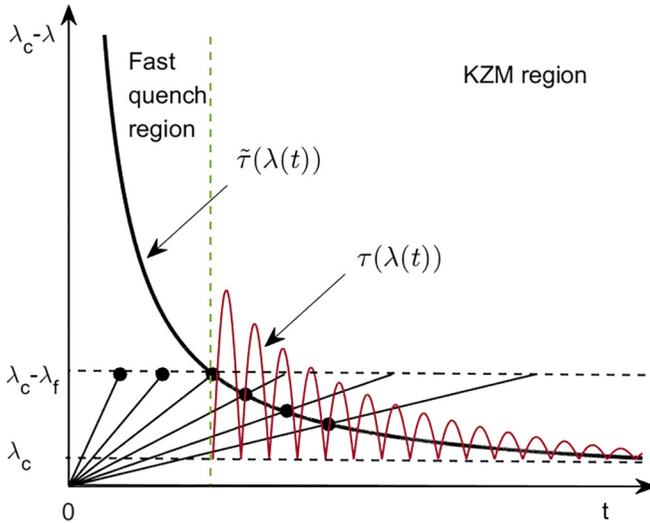
FIG. 1. Universal breakdown of KZM in a fast nonequilibrium phase transition. The effective relaxation time $\tilde{\tau}(\lambda(t))$ should be the time average of the real relaxation time $\tau(\lambda(t))$ (red line). The freeze-out time determined by equating the time elapsed after crossing the phase transition to average relaxation time (large black dot). In fast quench regions with finite depth λ_f, the quench is saturated at a fixed equilibrium relaxation time $\tilde{\tau}(\lambda_f)$, which we will explain later.

numerical simulations and experiments have recently demonstrated that KZM can be applied to some nonequilibrium phase transitions involving steady states [24–29]. Such scenarios are characterized by nonconservation of energy and particle number, and arise, for instance, in exciton-polariton systems [30] and directed percolation [31,32]. These results thus extend the universality of KZM to nonequilibrium systems in the limit of slow quenches.

Here, we consider universal scaling laws with arbitrary quench rates in another large class of nonequilibrium phase transitions: the periodic field-oscillatory dynamic phase transitions, which have been studied in a wide range of systems [33–37]. The unique property of this kind of nonequilibrium phase transition is that the periodic field phase transition requires a continuous input of energy from the external field to maintain the phase transition state. In this phase transition, all the quantities change periodically. For example, the relaxation time varies according to $\tau = \frac{\tau_0}{|1-\lambda|\cos(\Omega t)|/\lambda_c|^{z\nu}}$. Although detailed balance is not satisfied, it is believed that an average critical exponent can represent the phase transition behavior [38]. Even if the relaxation time oscillates continuously, the freezing of the system can be determined by the average relaxation time $\tilde{\tau}$, making it possible to verify the universal scaling laws with these average critical exponents, see Fig. 1. An analysis of the the quasinormal modes (QNMs) can provide the real relaxation time with periodic oscillation. However, whether the critical behavior of periodically driven phase transitions can be described by mean critical exponents is controversial. In this nonequilibrium system, we investigate whether KZM is satisfied for slow quenches and whether the number of defects under fast quenches exhibits a universal scaling behavior with the quench rate or the final value of the

control parameter. We establish the validity of the nonequilibrium scaling relations with the average critical exponents.

We focus on the response of a superconductor or superfluid to an applied periodic field that is governed by the proximity of the applied field to the critical magnetic field of the superconductor or the critical velocity of the superfluid [39,40]. The response is bidirectional in the periodic field system. Only when the suppression rate of the increasing field is the same as the recovery rate of the decreasing field, the system reaches an nonequilibrium steady state. To investigate the significant response of this order parameter to the external field [41–43], we use a holographic setting, the so-called AdS/CFT duality, for numerical experiments. This duality arises from Maldacena's celebrated conjecture in string theory [44] and establishes a surprising equivalence relationship between the high dimensional classical gravitational field and the low dimensional strongly coupled quantum field without gravity [45,46]. Holographic duality offers a novel first-principles perspective in condensed matter physics and finds extensive applications in the exploration of quantum many-body systems exhibiting superfluidity, superconductivity, and supersolid behavior [47–50].

II. HOLOGRAPHIC SETUP AND NUMERICAL METHOD

Holographic duality has been extensively employed in studying KZM in equilibrium phase transitions [51–54]. In particular, recent research using holographic models has uncovered a new universal scaling behavior in the fast quenching regime beyond KZM [55]. This behavior has been simultaneously validated in both the ϕ^4 model and the quantum Ising chain model [53], further highlighting the significant importance of holographic models in providing a deeper understanding of condensed matter physics and emphasizing their relevance in explaining complex phenomena.

We employ a bottom-up holographic model, in which $(2+1)$-dimensional superconductivity/superfluidity is described by an Abelian-Higgs model living in a $(3+1)$-dimensional asymptotically anti-de Sitter (AdS) black hole spacetime. In this model, the AdS black hole couples with a charged scalar field and a U(1) gauge field. Consequently, the action can be written as

$$S = \int d^4x \sqrt{-g} \left[-\frac{1}{4}F_{\mu\nu}F^{\mu\nu} - |\partial_\mu \Psi - iqA_\mu \Psi|^2 - m^2|\Psi|^2 \right].$$

(3)

Here, $F_{\mu\nu} = \partial_\mu A_\nu - \partial_\nu A_\mu$ is the Maxwell field strength with vector potential A_μ, which is coupled minimally to the scalar involving the charge q. Ψ is the complex scalar field with mass $m^2 = -2$. The background metric in the Eddington coordinate is $ds^2 = \frac{L}{z^2}[-f(z)dt^2 - 2dtdz + dx^2 + dy^2]$, with $f(z) = 1 - (z/z_h)^3$, and the Hawking temperature can be expressed as $T = 3/(4\pi z_h)$. We set a square boundary with periodic boundary conditions, where x and y are the spatial coordinates, and z is the extra radial dimension of the bulk. From the static holographic superconductor [48], the temperature can be controlled by the only dimensional parameter, the chemical potential μ, that satisfies $T/T_c = \mu_c/\mu$. As the chemical potential grows beyond a critical value $\mu_c = 4.07$, which means the temperature falls below the critical

temperature, the dual scalar field at the boundary exhibits a finite expectation value, i.e., the superconductor/superfluid order parameter $\langle O \rangle$. In this work, we fix the background temperature $T = 0.77T_c$, so we have a finite order parameter in the initial state without an external field.

Dynamic simulations can be conducted through numerical solutions of the equations of motion (EOM). These equations govern the behavior of bulk gauge and scalar fields, describing the equilibrium geometry within the bulk. They can be succinctly expressed as follows:

$$d_\nu F^{\mu\nu} = J^\mu = iq(\Psi^* D^\mu \Psi - \Psi D^\mu \Psi^*), \quad (4)$$

$$(-D^2 + m^2)\Psi = 0. \quad (5)$$

By imposing holographic periodic boundary conditions, we numerically solved these equations of motion. Specifically, we use high-order Runge-Kutta methods for accuracy and efficiency. Furthermore, in the z direction, we utilize the Chebyshev method, while in the x and y directions, the Fourier method was applied to address boundary conditions. For a 40×40 size system, we used a sufficiently accurate grid point of 300×300.

III. KIBBLE-ZUREK MECHANISM IN OSCILLATING DYNAMIC PHASE TRANSITION

A. Oscillating dynamic phase transition

We turn on the spatial gauge field component $A_{x,y}$ to induce the external driving force into the system. We take a sinusoidal form of the boundary conditions at $z = 0$,

$$A_x(t, z = 0) = \frac{E \sin(\Omega t)}{\Omega}. \quad (6)$$

The oscillating field along the x direction can be represented by the time derivative of the gauge field

$$E_x(t) = \partial_t A_x = E \cos(\Omega t). \quad (7)$$

Here, E is the amplitude, and Ω is the frequency of the applied field. With the fixed frequency $\Omega = 0.3\mu_c$, the finite amplitude E causes the system to enter a nonequilibrium oscillatory state, and the average order parameter decreases relative to the stable equilibrium state. This is an inevitable consequence of the equation of motion [56].

As shown in the upper panel in Fig. 2, when an oscillating field is added to the initial statically stable solution, the order parameters begin to oscillate, and the average value decreases gradually. Eventually, according to the amplitude of the field, a nonequilibrium steady state with a different mean value is reached. Our result shows that the critical value of the amplitude is $E_c = 0.705\mu_c$. The decay of the order parameters is related to the system's response to the external field.

The bottom left panel shows, separately, the increasing and decreasing velocities of the order parameters, defined as $|\Delta\langle O \rangle_\pm|$, with the rates defined as $v_\pm = \partial_t |\Delta\langle O \rangle_\pm|$. Since the decrease of the order parameter is accompanied by energy absorption, we refer to v_- as the absorption rate and v_+ as the release rate. At the beginning, when the order parameter is large enough, the system's response to the large field is significant, so the absorption rate is much larger than the release rate. With the decrease of the order parameter, the absorption rate
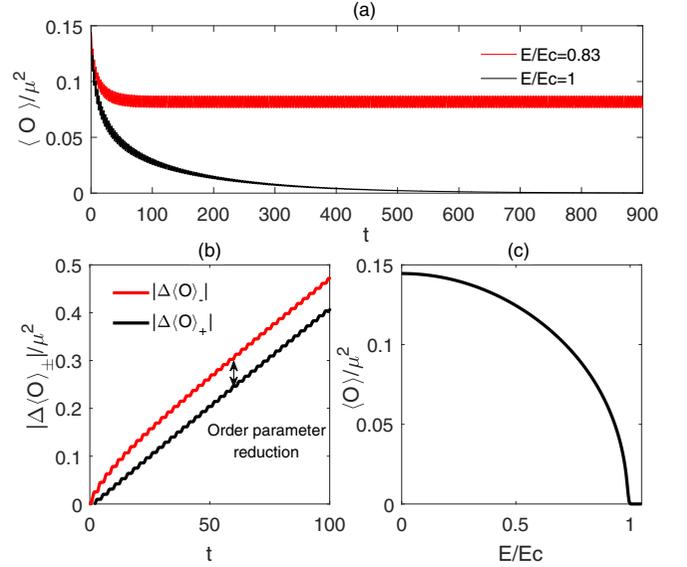

FIG. 2. (a) Evolution of order parameters in an external oscillating field. With the addition of the oscillating field, the order parameters gradually decrease and finally reach a nonequilibrium steady state. The red line has an amplitude lower than the critical field $E/E_c = 0.83$ and corresponds to an oscillatory steady state. The black line has an amplitude equal to the critical field $E/E_c = 1$ and shows the decay of the order parameter in the steady state. (b) In the case of $E/E_c = 0.83$, the red line represents the rate at which the order parameters fall in response to a large electric field, while the black line represents the rate at which the small electric field order parameters recover to rise. (c) Phase diagram of the final average order parameter as a function of the amplitude of the field. When the amplitude of the field is greater than the critical value, the system is completely disordered and enters the normal state.

gradually declines and finally becomes equal to the release rate. At this time, the total reduction of the order parameter can be obtained from the integral difference between the two rates. The bottom right panel shows the complete phase diagram for this fixed temperature and frequency. The corresponding value of each field intensity is the long-time average value of the order parameter at the nonequilibrium steady state. Therefore, although detailed balance cannot be satisfied, the critical behavior of this nonequilibrium phase transition can be expressed in terms of the average critical exponent.

B. Quenching process

To linearly traverse the critical point and establish the universal scaling behavior in the critical dynamics, we first prepare an initial state where the electric field is slightly larger than the critical value $E_i = E_c + dE_c$, and then linearly quench to an ordered phase with an electric field of $E_f < E_c$ in a finite quench time τ_Q. In doing so, $E(t) = E_c[1 - \epsilon(t)]$ and $\epsilon(t) = t/\tau_Q$. To dynamically break system symmetry, we introduce the noise into the scalar field's evolution process within the bulk by satisfying the statistical distributions $\langle s(t, x_i) \rangle = 0$ and $\langle s(t, x_i)s(t', x_j) \rangle = h\delta(t - t')\delta(x_i - x_j)$ for every 100 time steps, with the amplitude $h = 10^3$ [51,57].
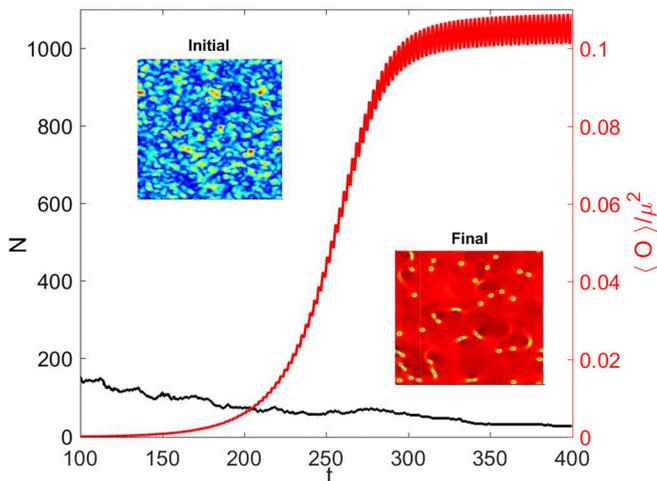
FIG. 3. Dynamic evolution of the nonequilibrium system with topological defects generated after a finite time quench with an oscillating field. The solid black line shows the number of topological defects with noise. The red line shows the evolution of the order parameter. The insets show the profile of order parameters before and after the freeze-out time, manifesting a distribution of vortices in the latter stage.

With the linear decrease of the amplitude of the electric field E, after crossing the frozen stage in the KZM description set by the freeze-out time, the system responds in the opposite direction to the previous description in Fig. 2, resulting in nonequilibrium symmetry breaking, and the order parameters gradually increase. As shown in Fig. 3, where we set $\tau_Q = 120$, the order parameters grow in an oscillatory fashion. At the same time, stable topological defects begin to appear. The distribution of topological defects can be identified in the built-in diagram at the lower right panel. We calculate the number of vortices by computing the phase winding numbers $N = \frac{1}{2\pi} \oint \nabla\theta \cdot dr$, where θ is the phase of the wave function which is defined as $\langle O \rangle = \psi = |\psi| e^{i\theta}$. To rule out contributions dominated by noise, the number of topological defects is determined after the order parameter starts to grow, acquiring a finite value. For each τ_Q, we fix the specific value $\langle O \rangle = 0.1$ and count the number of topological defects when this value of the order parameter is first reached $N_{t_f} = N_{\langle O \rangle = 0.1}$. The complete evolution process is shown in the movie in the Supplemental Material [58].

C. Kibble-Zurek mechanism in slow and fast region

According to our numerical results, in the slow quench region $\tau_Q > \tau_Q^c$, the number of vortices and quench rate satisfy the scaling $N \sim \tau_Q^{-1/2}$; see Fig. 4. The average critical exponents characterizing the order parameters in the oscillating field can be obtained by analyzing the quasinormal modes (QNMs) [38]. The specific method is to use the perturbation equation and correlation function of the system to get the relationship between the correlation length and relaxation time and the external field, and average the results under the steady state condition, so as to get the average critical exponents. According to the calculation, the average correlation-length critical exponent is $\nu = 1/2$ and the average dynamic critical
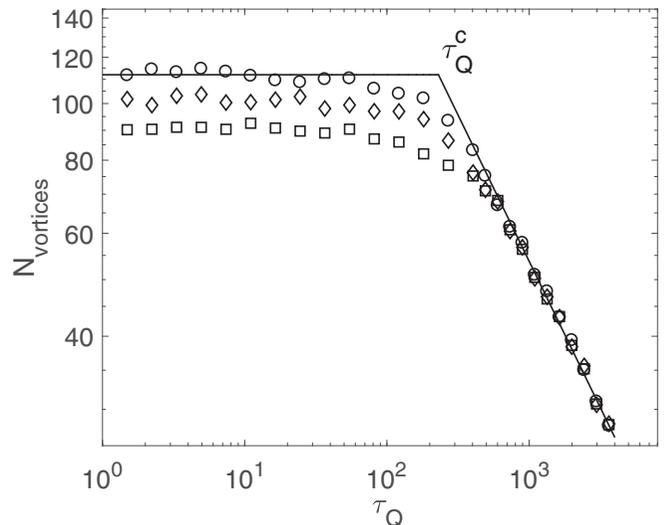

FIG. 4. The number of vortices N_{vortices} as a function of the quench time τ_Q in which the the electric field decays. For each τ_Q point, the number of topological defects is averaged over 100 trajectories. For slow quenches with $\tau_Q > 200$, the vortex number is consistent with the KZM scaling $N \sim \tau_Q^{-0.4832 \pm 0.0182}$. For fast quenches with $\tau_Q < 200$, the KZM is no longer satisfied, and the number of vortices does not vary with the quench rate. However, the value at the plateau scales universally with the amplitude of the quench, as shown from top to bottom, for the values of $E_f = 0E_c, 0.4E_c, 0.7Ec$, with the symbols $\bigcirc$, $\diamond$, $\square$, respectively.

exponent $z = 2$. Therefore, according to KZM, the topological defect density should follow a power law with exponent $-\frac{d\nu}{1+z\nu} = -1/2$. The validity of this prediction is confirmed by our results in the oscillating nonequilibrium phase transition. The nonequilibrium KZM result we obtain does not depend on the time average, which means that the mean critical exponent can indeed describe the nonequilibrium phase transition driven by the periodic field.

However, in the fast quench region where $\tau_Q < \tau_Q^c$, the KZM power-law scaling is no longer satisfied, and the number of vortices remains constant, saturating at the value of the instantaneous quench scenario. Recently, it has been observed that in specific systems, even in this fast quench region where the KZM breaks down, a universal scaling behavior still holds [52,53,55]. This theory relies on the fact that any realistic quench terminates at a finite value of E_f, which determines the lower limit of the relaxation time in the ordered phase. Accordingly, the freeze-out time should be set by $\hat{t} \sim \max\{\tau[E(\hat{t}), \tau(E_f)]\}$, see Fig. 1. Then, for fast quenches with $\tau(E_f) > \tau[E(\hat{t})]$, one finds a constant value of the freeze-out time, independent of τ_Q,

$$\hat{t} \sim \tau(E_f) \sim \epsilon_f^{-z\nu} = \epsilon_f^{-1}. \tag{8}$$

This explains the KZM breakdown and that the topological defect density saturates at a constant value which exhibits a distinct fast-quench universality. As shown in the right panel of Fig. 5(a), the freeze-out time in the oscillating system agrees with the prediction $t_f \sim \epsilon_f^{-1}$. The relationship between the vortex density and the final field value can be derived from this scaling. The average correlation length becomes
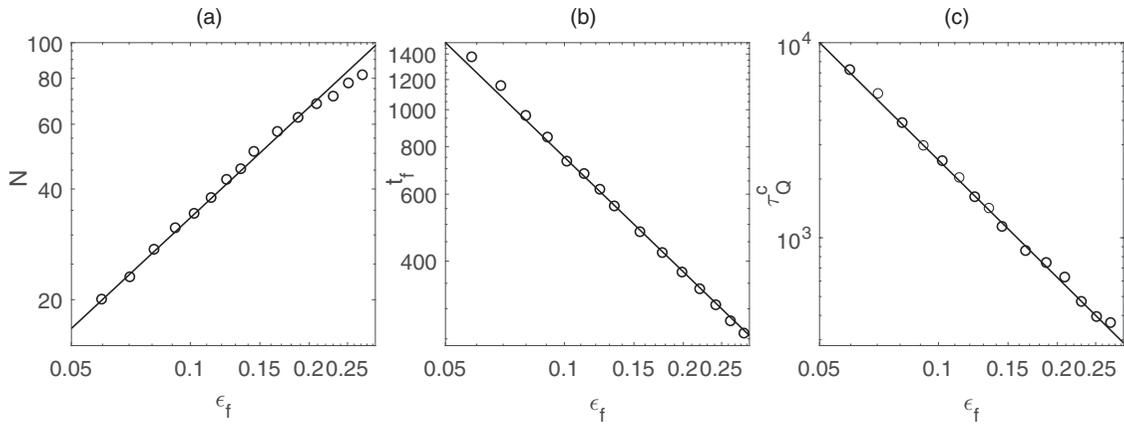
FIG. 5. Universal dynamics beyond KZM after a fast quench of the electric field with an oscillating dynamic phase transition. Panel (a) shows the linear scaling of the vortex number as a function of the final field intensity, i.e., $N \sim \epsilon_f^{1.003 \pm 0.0351}$. Panel (b) shows the dependence of the freeze-out time on ϵ_f, with data fitted to $\hat{t} \sim \epsilon_f^{-1.042 \pm 0.014}$. Panel (c) shows the dependence of the critical quench time on ϵ_f, with data fitted to $\tau_Q^c \sim \epsilon_f^{-1.985 \pm 0.031}$.

$\hat{\xi} = \xi(E_f)$ and sets the average length scale of the domain. The fast-quench vortex density scales universally as

$$n \sim \frac{1}{\xi(E_f)^d} \sim \epsilon_f^{d\nu} = \epsilon_f^1. \qquad (9)$$

Figure 5(b) validates this result, showing that the universal scaling beyond the KZM holds for the nonequilibrium phase transitions. The nonequilibrium relaxation time does not affect the distribution of freeze-out time. The critical quench rate can be defined by equating the time at which the quench ends at E_f, $t_f = \tau_Q^c(E_c - E_f)/E_c$. Then, $\tau_Q^c \sim \epsilon^{-(z\nu+1)} = \epsilon^{-2}$, as verified in Fig. 5(c).

IV. SUMMARY AND DISCUSSION

Our study contributes to understanding nonequilibrium phase transitions driven by a periodic oscillatory field. We shed light on the rich dynamics inherent in these transitions by validating the Kibble-Zurek mechanism for slow quenches and uncovering the universality of rapid quenches in the oscillating dynamic phase transition. Moreover, we demonstrate the validity of the time-average critical exponent in periodic dynamic phase transitions by establishing nonequilibrium KZM scaling laws independent of the time average. The exploration of these phenomena not only deepens our understanding of fundamental nonequilibrium physics but also paves the way for potential applications in areas such as materials science, quantum computing, and energy technologies. Our findings have significant implications for the applications of oscillating field-induced phase transitions in domains such as superconductivity, magnetism, and electric transport. The validation of the Kibble-Zurek mechanism and the discovery of rapid-quench universality provide insights into the dynamics of these transitions, which can be leveraged to design and optimize materials with desired properties. By tailoring the oscillatory field parameters and understanding the mechanisms driving the unconventional dynamics, we may achieve enhanced control over phase transitions, enabling advancements in superconducting technologies, magnetic devices, and systems for efficient electric and energy transport. In addition, by varying the parameters of the oscillatory fields, such as frequency, amplitude, or wave form, it may be possible to manipulate the formation and evolution of topological defects, leading to intriguing possibilities for controlling and engineering novel materials and functionalities.

[1] T. W. B. Kibble, Topology of cosmic domains and strings, J. Phys. A: Math. Gen. **9**, 1387 (1976).

[2] W. H. Zurek, Cosmological experiments in superfluid helium? Nature (London) **317**, 505508 (1985).

[3] A. del Campo and W. H. Zurek, Universality of phase transition dynamics: Topological defects from symmetry breaking, Int. J. Mod. Phys. A **29**, 1430018 (2014).

[4] I. Chuang, R. Durrer, N. Turok, and B. Yurke, Cosmology in the laboratory: Defect dynamics in liquid crystals, Science **251**, 1336 (1991).

[5] M. Mielenz, J. Brox, S. Kahra, G. Leschhorn, M. Albert, T. Schaetz, H. Landa, and B. Reznik, Trapping of topological-structural defects in coulomb crystals, Phys. Rev. Lett. **110**, 133004 (2013).

[6] G. Lamporesi, S. Donadello, S. Serafini, F. Dalfovo, and G. Ferrari, Spontaneous creation of Kibble–Zurek solitons in a bose–einstein condensate, Nat. Phys. **9**, 656 (2013).

[7] A. Polkovnikov, K. Sengupta, A. Silva, and M. Vengalattore, Colloquium: Nonequilibrium dynamics of closed interacting quantum systems, Rev. Mod. Phys. **83**, 863 (2011).

[8] C. N. Weiler, T. W. Neely, D. R. Scherer, A. S. Bradley, M. J. Davis, and B. P. Anderson, Spontaneous vortices in the formation of Bose-Einstein condensates, Nature (London) **455**, 948 (2008).

[9] J. Dziarmaga, J. Meisner, and W. H. Zurek, Winding up of the wave-function phase by an insulator-to-superfluid transition in a ring of coupled Bose-Einstein condensates, Phys. Rev. Lett. **101**, 115701 (2008).

[10] M. Kolodrubetz, B. K. Clark, and D. A. Huse, Nonequilibrium dynamic critical scaling of the quantum ising chain, Phys. Rev. Lett. **109**, 015701 (2012).

[11] P. C. Hohenberg and B. I. Halperin, Theory of dynamic critical phenomena, Rev. Mod. Phys. **49**, 435 (1977).

[12] M. J. Bowick, L. Chandar, E. A. Schiff, and A. M. Srivastava, The cosmological Kibble mechanism in the laboratory: String formation in liquid crystals, Science **263**, 943 (1994).

[13] P. C. Hendry, N. S. Lawson, R. A. M. Lee, P. V. E. McClintock, and C. D. H. Williams, Generation of defects in superfluid 4he as an analogue of the formation of cosmic strings, Nature (London) **368**, 315 (1994).

[14] V. M. H. Ruutu, V. B. Eltsov, A. J. Gill, T. W. B. Kibble, M. Krusius, Y. G. Makhlin, B. Plaçais, G. E. Volovik, and W. Xu, Vortex formation in neutron-irradiated superfluid ^{3}He as an analogue of cosmological defect formation, Nature (London) **382**, 334 (1996).

[15] M. E. Dodd, P. C. Hendry, N. S. Lawson, P. V. E. McClintock, and C. D. H. Williams, Nonappearance of vortices in fast mechanical expansions of liquid ^{4}He through the lambda transition, Phys. Rev. Lett. **81**, 3703 (1998).

[16] L. E. Sadler, J. M. Higbie, S. R. Leslie, M. Vengalattore, and D. M. Stamper-Kurn, Spontaneous symmetry breaking in a quenched ferromagnetic spinor Bose–Einstein condensate, Nature (London) **443**, 312 (2006).

[17] N. Navon, A. L. Gaunt, R. P. Smith, and Z. Hadzibabic, Critical dynamics of spontaneous symmetry breaking in a homogeneous bose gas, Science **347**, 167 (2015).

[18] J.-M. Cui, Y.-F. Huang, Z. Wang, D.-Y. Cao, J. Wang, W.-M. Lv, L. Luo, A. del Campo, Y.-J. Han, C.-F. Li, and G.-C. Guo, Experimental trapped-ion quantum simulation of the Kibble-Zurek dynamics in momentum space, Sci. Rep. **6**, 33381 (2016).

[19] A. Keesling, A. Omran, H. Levine, H. Bernien, H. Pichler, S. Choi, R. Samajdar, S. Schwartz, P. Silvi, S. Sachdev, P. Zoller, M. Endres, M. Greiner, V. Vuletić, and M. D. Lukin, Quantum Kibble–Zurek mechanism and critical dynamics on a programmable rydberg simulator, Nature (London) **568**, 207 (2019).

[20] J.-M. Cui, F. J. Gómez-Ruiz, Y.-F. Huang, C.-F. Li, G.-C. Guo, and A. del Campo, Experimentally testing quantum critical dynamics beyond the Kibble–Zurek mechanism, Commun. Phys. **3**, 44 (2020).

[21] Y. Bando, Y. Susa, H. Oshiyama, N. Shibata, M. Ohzeki, F. J. Gómez-Ruiz, D. A. Lidar, S. Suzuki, A. del Campo, and H. Nishimori, Probing the universality of topological defect formation in a quantum annealer: Kibble-Zurek mechanism and beyond, Phys. Rev. Res. **2**, 033369 (2020).

[22] A. D. King, S. Suzuki, J. Raymond, A. Zucca, T. Lanting, F. Altomare, A. J. Berkley, S. Ejtemaee, E. Hoskinson, S. Huang, E. Ladizinsky, A. J. R. MacDonald, G. Marsden, T. Oh, G. Poulin-Lamarre, M. Reis, C. Rich, Y. Sato, J. D. Whittaker, J. Yao *et al.*, Coherent quantum annealing in a programmable 2,000 qubit ising chain, Nat. Phys. **18**, 1324 (2022).

[23] K. Du, X. Fang, C. Won, C. De, F.-T. Huang, W. Xu, H. You, F. J. Gómez-Ruiz, A. del Campo, and S.-W. Cheong, Kibble–Zurek mechanism of ising domains, Nat. Phys. **19**, 1495 (2023).

[24] S. Ducci, P. L. Ramazza, W. González-Viñas, and F. T. Arecchi, Order parameter fragmentation after a symmetry-breaking transition, Phys. Rev. Lett. **83**, 5210 (1999).

[25] S. Casado, W. González-Viñas, H. Mancini, and S. Boccaletti, Topological defects after a quench in a Bénard-Marangoni convection system, Phys. Rev. E **63**, 057301 (2001).

[26] S. Casado, W. González-Viñas, and H. Mancini, Testing the Kibble-Zurek mechanism in Rayleigh-Bénard convection, Phys. Rev. E **74**, 047101 (2006).

[27] S. Casado, W. González-Viñas, S. Boccaletti, P. L. Ramazza, and H. Mancini, The birth of defects in pattern formation: Testing of the Kibble-Zurek mechanism, Eur. Phys. J.: Spec. Top. **146**, 87 (2007).

[28] M. A. Miranda, J. Burguete, W. González-Viñas, and H. Mancini, Exploring the Kibble-Zurek mechanism in a secondary bifurcation, Int. J. Bifurcation Chaos **22**, 1250165 (2012).

[29] M. A. Miranda, J. Burguete, H. Mancini, and W. González-Viñas, Frozen dynamics and synchronization through a secondary symmetry-breaking bifurcation, Phys. Rev. E **87**, 032902 (2013).

[30] A. Zamora, G. Dagvadorj, P. Comaron, I. Carusotto, N. P. Proukakis, and M. H. Szymańska, Kibble-Zurek mechanism in driven dissipative systems crossing a nonequilibrium phase transition, Phys. Rev. Lett. **125**, 095301 (2020).

[31] C. J. O. Reichhardt, A. del Campo, and C. Reichhardt, Kibble-Zurek mechanism for nonequilibrium phase transitions in driven systems with quenched disorder, Commun. Phys. **5**, 173 (2022).

[32] S. Maegochi, K. Ienaga, and S. Okuma, Kibble-Zurek mechanism for dynamical ordering in a driven vortex system, Phys. Rev. Lett. **129**, 227001 (2022).

[33] S. W. Sides, P. A. Rikvold, and M. A. Novotny, Kinetic ising model in an oscillating field: Finite-size scaling at the dynamic phase transition, Phys. Rev. Lett. **81**, 834 (1998).

[34] T. Tomé and M. J. de Oliveira, Dynamic phase transition in the kinetic ising model under a time-dependent oscillating field, Phys. Rev. A **41**, 4251 (1990).

[35] Y. Yüksel, E. Vatansever, U. Akıncı, and H. Polat, Nonequilibrium phase transitions and stationary-state solutions of a three-dimensional random-field ising model under a time-dependent periodic external field, Phys. Rev. E **85**, 051123 (2012).

[36] H. P. O. Collado, G. Usaj, C. A. Balseiro, D. H. Zanette, and J. Lorenzana, Dynamical phase transitions in periodically driven Bardeen-Cooper-Schrieffer systems, Phys. Rev. Res. **5**, 023014 (2023).

[37] A. Eckardt, C. Weiss, and M. Holthaus, Superfluid-insulator transition in a periodically driven optical lattice, Phys. Rev. Lett. **95**, 260404 (2005).

[38] H.-B. Zeng and H.-Q. Zhang, Universal critical exponents of nonequilibrium phase transitions from holography, Phys. Rev. D **98**, 106024 (2018).

[39] K. Holczer, O. Klein, G. Grüner, J. D. Thompson, F. Diederich, and R. L. Whetten, Critical magnetic fields in the superconducting state of K_3C_{60}, Phys. Rev. Lett. **67**, 271 (1991).

[40] J. S. Langer and M. E. Fisher, Intrinsic critical velocity of a superfluid, Phys. Rev. Lett. **19**, 560 (1967).

[41] C. P. Herzog, P. K. Kovtun, and D. T. Son, Holographic model of superfluidity, Phys. Rev. D **79**, 066002 (2009).

[42] E. Nakano and W.-Y. Wen, Critical magnetic field in a holographic superconductor, Phys. Rev. D **78**, 046004 (2008).

[43] W.-C. Yang, C.-Y. Xia, H.-B. Zeng, M. Tsubota, and J. Zaanen, Motion of a superfluid vortex according to holographic quantum dissipation, Phys. Rev. B **107**, 144511 (2023).

[44] J. Maldacena, The large-N limit of superconformal field theories and supergravity, Int. J. Theor. Phys. **38**, 1113 (1999).

[45] S. Gubser, I. Klebanov, and A. Polyakov, Gauge theory correlators from non-critical string theory, Phys. Lett. B **428**, 105 (1998).

[46] E. Witten, Anti de sitter space and holography, arXiv:hep-th/9802150 [hep-th]

[47] C. P. Herzog, Lectures on holographic superfluidity and superconductivity, J. Phys. A: Math. Theor. **42**, 343001 (2009).

[48] S. A. Hartnoll, C. P. Herzog, and G. T. Horowitz, Building a holographic superconductor, Phys. Rev. Lett. **101**, 031601 (2008).

[49] M. Baggioli and G. Frangi, Holographic supersolids, J. High Energy Phys. 06 (2022) 152.

[50] W.-C. Yang, C.-Y. Xia, H.-B. Zeng, and H.-Q. Zhang, Phase separation and exotic vortex phases in a two-species holographic superfluid, Eur. Phys. J. C **81**, 21 (2021).

[51] J. Sonner, A. del Campo, and W. H. Zurek, Universal far-from-equilibrium dynamics of a holographic superconductor, Nat. Commun. **6**, 7406 (2015).

[52] P. M. Chesler, A. M. García-García, and H. Liu, Defect formation beyond Kibble-Zurek mechanism and holography, Phys. Rev. X **5**, 021015 (2015).

[53] H.-B. Zeng, C.-Y. Xia, and A. del Campo, Universal breakdown of Kibble-Zurek scaling in fast quenches across a phase transition, Phys. Rev. Lett. **130**, 060402 (2023).

[54] C.-Y. Xia and H.-B. Zeng, Winding up a finite size holographic superconducting ring beyond Kibble-Zurek mechanism, Phys. Rev. D **102**, 126005 (2020).

[55] C.-Y. Xia and H.-B. Zeng, Kibble zurek mechanism in rapidly quenched phase transition dynamics, arXiv:2110.07969 [cond-mat.stat-mech].

[56] W.-J. Li, Y. Tian, and H. Zhang, Periodically driven holographic superconductor, J. High Energy Phys. 07 (2013) 030.

[57] H.-B. Zeng, C.-Y. Xia, and H.-Q. Zhang, Topological defects as relics of spontaneous symmetry breaking from black hole physics, J. High Energy Phys. 03 (2021) 136.

[58] See Supplemental Material at http://link.aps.org/supplemental/10.1103/PhysRevB.108.174518 for the movie shows the complete quenching process, the vortex generation process when the periodic external field amplitude drops from the critical value to the final quenching value.

Correction: The omission of the "Contact author" label in the footnote for the last author has been fixed.